J|A|C|S ARTICLES

Published on Web 05/28/2009

Dissociation of Water During Formation of Anodic Aluminum Oxide

Zixue Su, Michael Bühl,* and Wuzong Zhou*

School of Chemistry, University of St. Andrews, North Haugh, St. Andrews, Fife KY16 9ST, U.K.

Received March 23, 2009; E-mail: buehl@st-andrews.ac.uk; wzhou@st-andews.ac.uk

Abstract: According to model computations at the B3LYP/6-311+G** level, an external electric field can facilitate the heterolytic dissociation of properly oriented water molecules significantly. Depending on the models used, the maximum predicted change of the dissociation energy in the field is ca. −3 to −4 kcal nm mol^{-1} V^{-1}, and decreases with the cosine of the angle between the external field and the breaking OH bond. These microscopic results can be related semiquantitatively to macroscopic observables from mechanistic studies on the pore formation of anodic aluminum oxide, thus lending support to the equifield strength model and field-enhanced water dissociation at the growing oxide surface that has been put forward in these studies.

Introduction

Porous anodic aluminum oxide (AAO), first reported 50 years ago,[1] has become a popular material in recent years as a template for fabrication of various nanotubes, nanowires, and porous films of other compositions,[2] and is now commercially available. However, the formation mechanism, including self-organization of honeycomb patterned pore arrays, is still not fully understood, although great efforts have been made by many groups.[3] The most recent development performed in these laboratories is an establishment of an equifield strength model for elucidating pore initiation, pore growth, hemispherical pore bottom, and self-ordering.[4] It has also been proposed that heterolytic dissociation of water at the electrolyte/oxide interface is the key factor for governing the porosity (P) of AAO films, in a very simple relation

$$P = 3/(n + 3) \tag{1}$$

where n is introduced to indicate the amount of water that dissociates per mole of Al_2O_3 that is dissolved at the same time, according to the following reaction:

$$Al_2O_3(s) + nH_2O(l) \rightarrow 2Al^{3+}(aq) + (3 + n - x)O^{2-}(s) + xOH^-(s) + (2n - x)H^+(aq) \tag{2}$$

From the observed porosities as function of the anodization conditions (in particular the applied voltage), an important prediction of this model is that the rate of this dissociation process at such a liquid/solid interface should increase with the strength of the applied electric field. Such water dissociation is even more important during anodization of titanium, since it has been discovered recently that the product of water dissociation, OH^-, forms a hydroxide layer in between the oxide layer and the metal substrate.[4c] Generally speaking, field-enhanced water dissociation may play an important role in many corrosion processes but has not been extensively investigated. We now address this fundamental, important, and long-standing problem by a combined methodology of computational and experimental chemistry.

For this purpose, we used quantum chemistry to model the OH bond strength of water as a function of the applied external electric field. Inclusion of such an electric field in the computations is straightforward, and a number of ab initio and density functional theory (DFT) studies have addressed the field-dependence of structures,[5] dipole moments,[6] bond strengths,[7] or reactivities[8] of molecules or solids. Field effects on the

(1) Keller, F.; Hunter, M. S.; Robinson, D. L. *J. Electrochem. Soc.* **1953**, *100*, 411–419.
(2) (a) Su, Z. X.; Sha, J.; Pan, G. W.; Liu, J. X.; Yang, D. R.; Dickinson, C.; Zhou, W. Z. *J. Phys. Chem. B* **2006**, *110*, 1229–1234. (b) Fu, J.; Cherevko, S.; Chung, C. H. *Electrochem. Commun.* **2008**, *10*, 514–518. (c) Yanagishita, T.; Nishio, K.; Masuda, H. *Adv. Mater.* **2006**, *17*, 2241–2243.
(3) (a) Masuda, H.; Fukuda, K. *Science* **1995**, *268*, 1466–1468. (b) De Graeve, I.; Terryn, H.; Thompson, G. E. *J. Electrochem. Soc.* **2003**, *150*, B158–B165. (c) Kashi, M. A.; Ramazani, A. *J. Phys. D: Appl. Phys.* **2005**, *38*, 2396–2399. (d) Li, A. P.; Müller, F.; Birner, A.; Nielsch, K.; Gösele, U. *J. Appl. Phys.* **1998**, *84*, 6023–6026. (e) Jessensky, O.; Müller, F.; Gösele, U. *Appl. Phys. Lett.* **1998**, *72*, 1173–1175. (f) Singh, G. K.; Golovin, A. A.; Aranson, I. S. *Phys. Rev. B* **2006**, *73*, 205422.
(4) (a) Su, Z. X.; Zhou, W. Z. *Adv. Mater.* **2008**, *20*, 3663–3667. (b) Su, Z. X.; Hähner, G.; Zhou, W. Z. *J. Mater. Chem.* **2008**, *18*, 5787–5795. (c) Su, Z. X.; Zhou, W. Z. *J. Mater. Chem.* **2009**, *19*, 2301–2309.
(5) Tielens, F.; Gracia, L.; Polo, V.; Andres, J. *J. Phys. Chem. A* **2007**, *111*, 13255–13263.
(6) Rai, D.; Joshi, H.; Kulkarni, A. D.; Gejji, S. P.; Pathak, R. K. *J. Phys. Chem. A* **2007**, *111*, 9111–9121.
(7) (a) Rozas, I.; Alkorta, I.; Elguero, J. *Chem. Phys. Lett.* **1997**, *275*, 423–428. (b) Mata, I.; Molins, E.; Alkorta, E.; Espinosa, E. *J. Chem. Phys.* **2009**, *130*, 044104.
(8) (a) Ramos, M.; Alkorta, I.; Elguero, J.; Golubev, N. S.; Denisov, G. S.; Benedict, H.; Limbach, H. H. *J. Phys. Chem. A* **1997**, *101*, 9791–9800. (b) Shaik, S.; de Visser, S. P.; Kumar, D. *J. Am. Chem. Soc.* **2004**, *126*, 11746–11749. (c) Marcos, E.; Anglada, J. M.; Crehuet, R. *Phys. Chem. Chem. Phys.* **2008**, *10*, 2442–2450. (d) McEwen, J.-S.; Gaspard, P.; Mittendorfer, F.; de Bocarme, T. V.; Kruse, N. *Chem. Phys. Lett.* **2008**, *452*, 133–138.

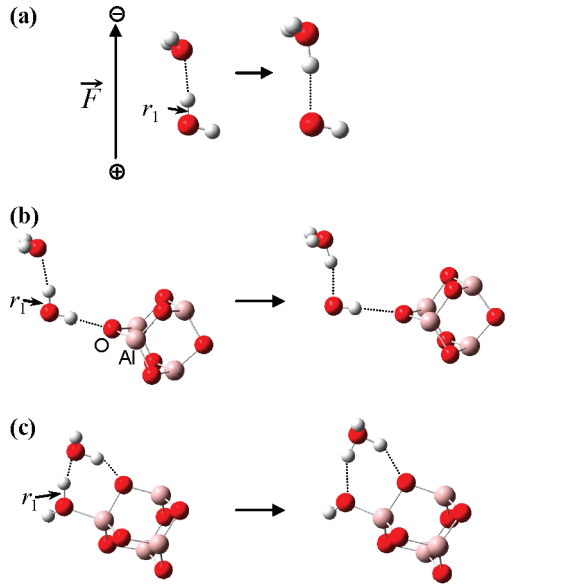

Figure 1. Models to study the effect of an electric field on the dissociation of an OH bond (labeled r_1) in a water molecule: (a) water dimer, (b) water dimer donating a H bond to an Al_4O_6 cluster, (c) water dimer coordinated via the O atom to an Al_4O_6 cluster.

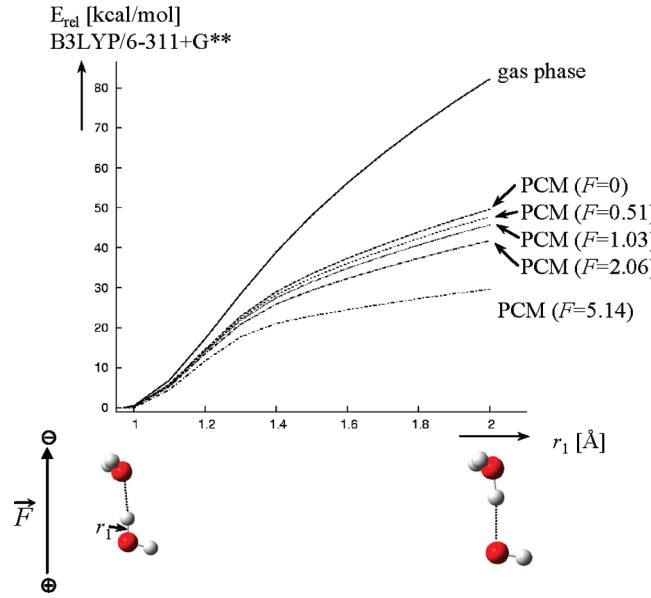

Figure 2. Dissociation profiles for the OH bond in the water dimer ($\alpha = 0$) in the gas phase and in a polarizable continuum ($\epsilon = 6$, F in V nm^{-1}).

H-bond network of liquid water[9] and on mobility of hydronium ions therein[10] have been modeled theoretically, but to our knowledge, the question of the bond strength of water in an external field has not been addressed yet.

First-principles predictions of thermodynamic and kinetic parameters of heterolytic bond dissociations in polar condensed media are a daunting challenge. The simplest possible model system for the effect under scrutiny is the water dimer dissociating into an $OH^-H_3O^+$ ion pair, where the hydroxide would remain bound at the oxide surface, later migrating across the oxide layer to the oxide/metal interface, and the hydronium ion would eventually be released into the electrolyte solution. For this and somewhat more elaborate models (see Figure 1), we evaluated heterolytic dissociation profiles quantum-mechanically at suitable levels (e.g., B3LYP/6-311+G(d,p) in a polarizable continuum) in the presence of an external field suitably aligned with the breaking OH bond.

Computational Details

The systems shown in Figure 1 were first fully optimized without electric field in the gas phase at the B3LYP/6-311+G** level,[11,12] where all are true minima. Subsequently, dissociation profiles were computed at the same level by elongating the OH bond successively in steps of 0.1 Å and optimizing all other geometrical parameters of the water dimer moiety, except for the O−H···O bond angle, which was kept fixed at the value of the respective minimum (to prevent the forming H_3O^+ from "bending back" to the hydroxide by closing this angle). For the cluster models, the Al_4O_6 moieties were also kept fixed in their fully optimized structures. Next, single-point energy computations were performed on these partially optimized gas-phase structures employing the polarizable continuum model (PCM) by Tomasi and co-workers,[13] using a dielectric constant of $\epsilon = 6$ (see below) and Merz−Kollman atomic radii (together with explicit hydrogens) for the construction of the cavity. Finally, these single-point energy computations were repeated in the presence of an electric field of a given strength F and fixed orientation with respect to the breaking OH bond. The stabilization energies ΔE were evaluated as differences between the latter energies (at an O···H distance of 2.0 Å) and those in the field-free cases, where a negative sign denotes a stabilization in the field. For the free water dimer, the same protocol was followed also at the MP2/6-311+G** level. All computations were performed using the Gaussian03 program package.[14]

Results

To illustrate the dependence of the ΔE values on the strength of the external field, the dissociation profiles for perfect alignment of field and OH bond are plotted for the water dimer in Figure 2. Due to the imperfections of this simplistic model for water dissociation, the resulting profiles themselves are not realistic in a quantitative sense. What is intersting and significant, however, is the extent of the lowering of the energies with increasing field strength. In actual liquid water, an OH distance of ca. 1.8 Å can be considered as effectively broken. This is evident, for instance, from constrained Car−Parrinello molecular dynamics simula-

(9) Suresh, S. J.; Satish, A. V. *J. Chem. Phys.* **2006**, *124*, 074506.
(10) Choe, Y.-K.; Tsuchida, E.; Ikeshoji, T. *J. Chem. Phys.* **2007**, *126*, 154510.
(11) (a) Becke, A. D. *J. Chem. Phys.* **1993**, *98*, 5648–5642. (b) Lee, C.; Yang, W.; Parr, R. G. *Phys. Rev. B* **1988**, *37*, 785–789. (c) Krishnan, R.; Binkley, J. S.; Seeger, R.; Pople, J. A. *J. Chem. Phys.* **1980**, *72*, 650–654. (d) Clark, T.; Chandrasekhar, J.; Spitznagel, G. W.; Schleyer, P. v. R. *J. Comput. Chem.* **1983**, *4*, 294–301.
(12) This and similar levels are well suited to study properties of water such as dipole moment, binding energy of the dimer, etc., see, e.g.: (a) Koch, W.; Holthausen, M. C. *A Chemist's Guide to Density Functional Theory*, 2nd. Ed.; Wiley-VCH: Weinheim, 2001. Also, the experimental proton affinity of water is reproduced within 0.5 kcal mol^{-1} at the B3LYP/6-311+G(d,p) level: (b) DiLabio, G. A.; Pratt, D. A.; LoFaro, A. D.; Wright, J. S. *J. Phys. Chem. A* **1999**, *103*, 1653–1661.
(13) (a) Miertus, S.; Scrocco, E.; Tomasi, J. *Chem. Phys.* **1981**, *55*, 117–129. (b) Mennucci, B.; Tomasi, J. *J. Chem. Phys.* **1997**, *106*, 5151–5158. (c) Barone, V.; Cossi, M.; Tomasi, J. *J. Chem. Phys.* **1997**, *107*, 3210–3221.
(14) Frisch, M. J.; et al. *Gaussian 03, revision E01*; Gaussian, Inc.: Pittsburgh, PA, 2003.

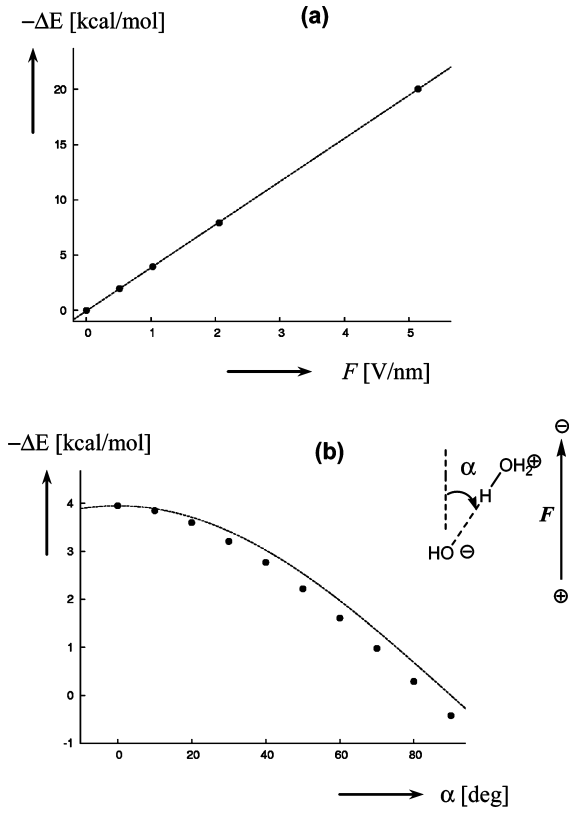

Figure 3. Stabilization energy ΔE of the water dimer (at $r_1 = 2.0$ Å and $\epsilon = 6$) as a function of (a) the field strength F (for $\alpha = 0$) and (b) the angle α (at $F = 1.03$ V nm^{-1}).

tions of the bulk liquid, where the free energy of O−H dissociation starts to level off at such a distance,[15] and the well-known hopping mechanism for proton transport sets in. To be on the safe side, we assumed a distance of 2.0 Å for full dissociation and evaluated the stabilization energy with respect to the field-free case, ΔE, at this value for r_1.[16] Figure 3a shows the almost perfect linearity between the resulting ΔE values and the field strength F in this orientation. If the field is aligned such that the dissociating O and H atoms are at the positive and negative poles, respectively, ΔE is negative.

The orientation dependence of ΔE as function of α is shown for the water dimer in Figure 3b, employing an intermediate value of F (1.03 V nm^{-1}). The computed data (black dots) can be approximated reasonably well by a simple cosine function (solid line).[17] Assuming the same holds for all field strengths affords the expression in eq 3:

$$\Delta E \approx c_1 F \cos \alpha \qquad (3)$$

where c_1 is a positive constant. A linear fit of ΔE values obtained at $F = 0.51$, 1.03, 2.06, and 5.14 V nm^{-1} yields $c_1 = 3.90$ kcal nm mol^{-1} V^{-1}.[18,19] The choice of ϵ in these computations is not overly critical. For instance, for the water dimer at $\alpha = 0$, using $\epsilon = 78.4$ instead of 6 yields $c_1 = 4.03$ kcal nm mol^{-1} V^{-1} instead of 3.90 kcal nm mol^{-1} V^{-1}. Essentially the same value, 3.97 kcal nm mol^{-1} V^{-1}, is obtained at the MP2/6-311+G(d,p) level.

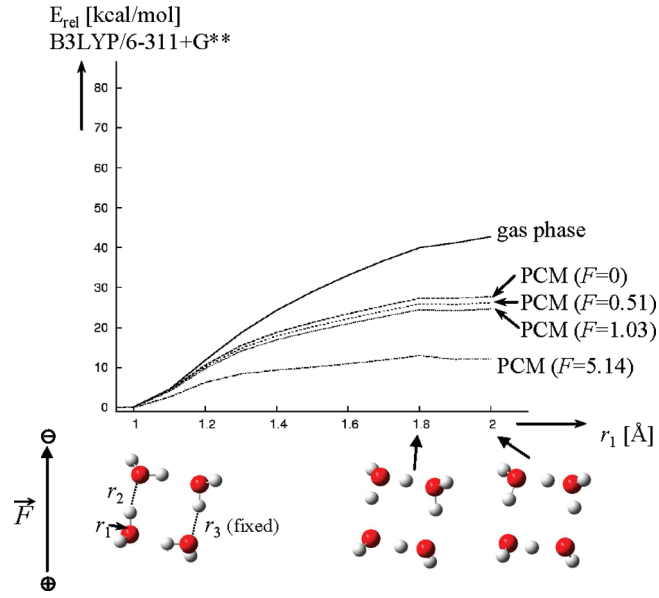

Figure 4. Dissociation profiles for an OH bond in the water tetramer in the gas phase and in a polarizable continuum ($\epsilon = 6$, F in V nm^{-1}).

The heterogeneous systems in the actual AAO process pose the additional complication that the microstructure of the porous aluminum oxide at the interface with the solution is rather ill-defined. DFT computations for an ideal periodic (0001) surface of α-Al_2O_3 have identified two favorite bonding modes of water at high coverage, namely donating an OH bond to a surface O atom or coordinating via O to an Al atom of the surface.[20] We have modeled this situation by attaching the dissociating water dimer in a corresponding manner to an Al_4O_6 cluster (which had been used before as simple alumina model[21]), see Figure 1b,c. The c_1 values obtained in these cases are 4.01 and 3.29 kcal nm mol^{-1} V^{-1}, respectively, i.e., qualitatively very similar to that obtained for the free water dimer.

In order to model effects of explicit hydration on the dissociation profile, we also studied the cyclic water tetramer in an analogous fashion. Starting from the S_4 symmetric minimum and elongating r_1 successively (see Figure 4), it was necessary to fix the opposite O···H distance (r_3 in Figure 4), in order to prevent a cyclic concerted transfer of the four bridging H atoms, which would eventually restore the neutral water tetramer rather than maintain the desired $H_3O_2^-$·$H_5O_2^+$ ion pair. No angle constraint was imposed in this case.

For this tetramer model, H transfer effectively occurs at $r_1 = 1.8$ Å, at which point the two unsymmetrical OH···O bonds at the "upper" and "lower" sides (referring to the orientation depicted at the bottom of Figure 4) invert, i.e., where they switch to the respective O···HO orientations. Using the same fitting procedure as for the water dimer, $c_1 = 2.96$ kcal nm mol^{-1} V^{-1}

(15) (a) Trout, B. L.; Parrinello, M. *Chem. Phys. Lett.* **1998**, *288*, 343–347. (b) Sprik, M. *Chem. Phys.* **2000**, *258*, 139–150.
(16) The precise choice of this distance is not overly critical, as ΔE values differ typically by less than 10% when evaluated at, e.g., $r_1 = 1.8$ Å instead of 2.0 Å.
(17) Using $\cos^2 \alpha$ instead of a simple cosine as trial function affords a worse fit (not shown).
(18) 1 kcal nm mol^{-1} V^{-1} = 4.18 × 10^{-6} C m mol^{-1}. Error bars from linear regressions are all smaller than ±0.01 kcal nm mol^{-1} V^{-1}.
(19) Exactly the same value is obtained with 6-311++G(d,p) basis, i.e., including diffuse functions on H atoms.
(20) Ranea, V. A.; Schneider, W. F.; Carmichael, I. *Surf. Sci.* **2008**, *602*, 268–275.
(21) Wittbrodt, J. M.; Hase, W. L.; Schlegel, H. B. *J. Phys. Chem. B* **1998**, *102*, 6539–6548.

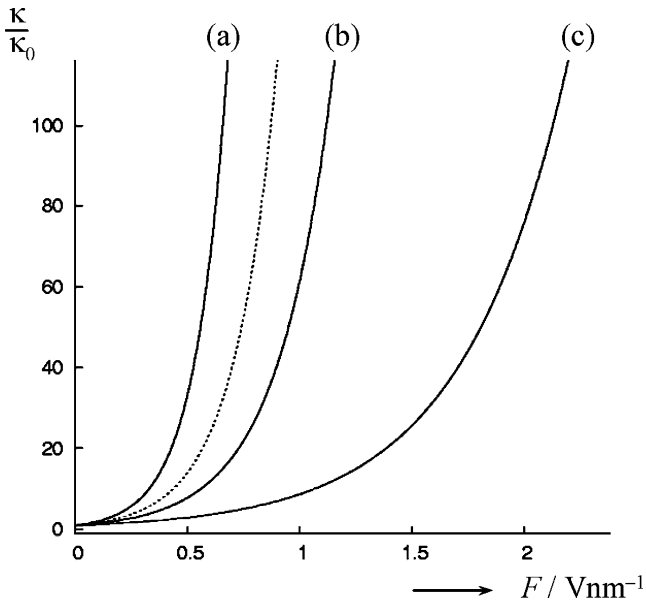

Figure 5. Plot of κ/κ_0 according to eq 4 ($T = 288$ K), using $c_1 = 4.01$ kcal nm mol^{-1} V^{-1}, and (a) $\alpha = 0$, (b) $\alpha = 54°$, and (c) $\alpha = 72°$ (the latter two correspond to the orientations in Scheme 1). Dotted line shows experimental estimate for $c_1 \cos \alpha = 3.0$ kcal nm mol^{-1} V^{-1} (see text).

is obtained for the tetramer. Note that, beyond $r_1 = 1.8$ Å, the potential energy curves in Figure 4 visibly level off, which is in good qualitative accord with sophisticated CPMD simulations.[15] In the field-free case, and using the dielectric constant of water, a dissociation energy around ca. 27 kcal/mol is obtained for our tetramer model, which can be compared with free energies of water dissociation in the bulk from CPMD/BLYP simulations (ca. 17 kcal/mol) and experiment (21.4 kcal/mol, see ref 15 and references cited therein). Given the simplicity of our model computations, and the neglect of temperature and entropy effects therein, the agreement with other theoretical and experimental data is actually quite reasonable. It is, however, not the dissociation energy as such that we attempt to model, but rather the effect of the electric field on it.

When the water-dissociation energy is lowered by an amount according to eq 3, and when all thermal and entropic contributions arising from the external field are neglected, the relative rate enhancement for the dissociation process is

$$\kappa/\kappa_0 = \exp[(c_1 F \cos \alpha)/RT] \tag{4}$$

where κ and κ_0 are the absolute rate constants with and without field, respectively. The ratios κ/κ_0 according to eq 4 are plotted in Figure 5 using the highest of the c_1 values as an upper limit, and a few representative values for α, estimated from idealized orientations of water molecules adsorbed on a surface (Scheme 1). These orientations refer to an extended planar surface perpendicular to the field (where X can be either O or Al), rather than to the simplistic models in Figure 1b,c. Evidently, the rate-enhancing effect of the field can be substantial, but should also be very sensitive to the orientation of the water molecules.

Discussion

In order to relate these microscopic results to the macroscopic observables, we now consider our working hypothesis for the anodization process in more detail. The total oxygen anionic

Scheme 1. Idealized Orientations of Water Molecules on a Surface

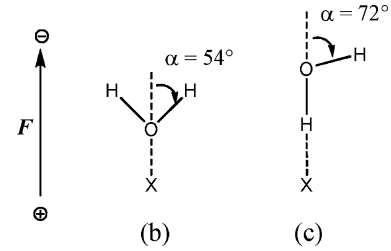

current j across the barrier oxide at the pore base consists of two parts, j_{oxide} from the electric-field enhanced dissolution of the oxide at the oxide/electrolyte interface, and j_{water} from the dissociation of water

$$j = j_{\text{water}} + j_{\text{oxide}} \tag{5}$$

where $j_{\text{water}}/j_{\text{oxide}} = n/3$ (n is defined by eq 2), since the current density is proportional to the anions created from the surface reactions. The porosity P of the anodic oxide film should be related to these current densities according to

$$P = \frac{3}{n + 3} = \frac{j_{\text{oxide}}}{j_{\text{oxide}} + j_{\text{water}}} = \frac{j_{\text{oxide}}}{j} \tag{6}$$

and

$$\frac{j_{\text{water}}}{j} = \frac{n}{n + 3} = 1 - \frac{3}{n + 3} = 1 - p \tag{7}$$

The oxygen-anion current attributed to the dissociation of water, j_{water}, should have the same relationship with the local electric field strength F at the oxide/electrolyte interface as the dissociation rate of water (eq 4). Neglecting the temperature change due to the local heating at the barrier oxide layer, there is

$$j_{\text{water}}/j^0_{\text{water}} = \exp[(c_1 F \cos \alpha)/RT] \tag{8}$$

where j^0_{water} denotes the oxygen-anion current attributed to the dissociation of water in the field-free case.

The main difficulty is now to relate the externally applied voltage U to the local field strength F at the oxide/water interface. As the aluminum-oxide layer is sandwiched by two effective conductors, aluminum metal and electrolyte solution, it is reasonable to assume that essentially all the voltage U is acting across the oxide layer of thickness d_C. With this simple model, and using experimental data for j and P (which are given in Table 1) together with previously established empirical relationships, values for F can be deduced. Using these raw data (which are included in Table 1) to fit eq 8 affords 6.3 kcal nm mol^{-1} V^{-1} as first estimate for the factor $c_1 \cos \alpha$.

The data were derived as follows. The fraction j_{water} in the total current strength, j, is given by

$$j_{\text{water}} = j(1 - P) \tag{9}$$

as obtained from eq 7. An empirical relation between j and F has been derived previously, namely eq 17 in ref 4b

$$j = 7.94 \times 10^{-4} \exp(10.45F) \tag{10}$$

Table 1. Experimental Data of Anodization[a]

	U (V)	j (mA)	p (%)	j_{water}[b] (mA)	F[b] (V nm^{-1})	ref
1	5	0.39	35.0	0.254	0.588	22
2	10	0.80	20.1	0.638	0.656	22
3	20	1.85	13.6	1.600	0.736	22
4	30	3.29	10.8	2.934	0.790	22
5	40	5.45	9.4	4.938	0.838	22
6	20	2.0	17.5[b]	1.65	0.743	4b
7	30	3.0	13.6[b]	2.59	0.782	4b
8	40	5.5	9.4[b]	4.98	0.839	4b
9	40	5	10	4.50	0.83	23
10	110	30	3.3	29.0	1.0	23a

[a] T = 288 K. Applied voltage = U, measured current = j, field strength = E, and measured porosity = P. [b] Derived value, see text.

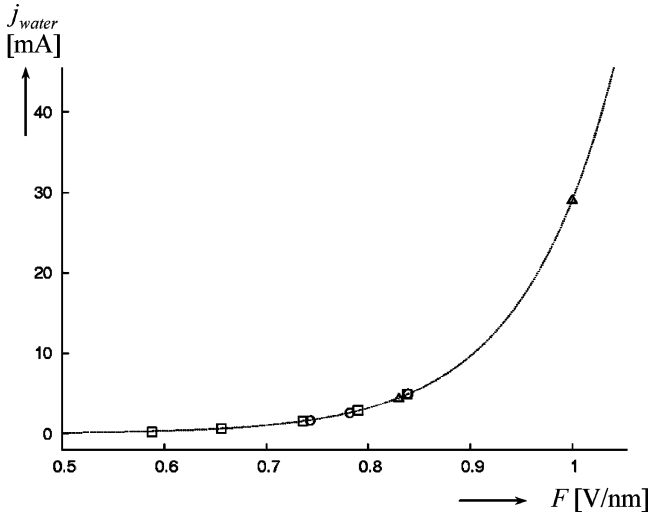

Figure 6. Plot of experimentally derived oxygen anion currents due to water dissociation, j_{water}, vs electric field strengths F, together with an exponential fit. Squares, circles, and triangles are based on data taken from refs 22, 4b, and 23, respectively.

where j and F are given in units of mA and V nm^{-1}, respectively. When no porosities have been reported, these have been estimated via the relationship derived in eq 19 of ref 4b

$$P = 21.3 \exp(-6.46F) \tag{11}$$

Figure 6 shows a plot of the resulting experimental j_{water} values versus the derived data for F collected in Table 1, together with a fit according to

$$j_{water} = j^0_{water} \exp[(c_1 F \cos \alpha)/RT] \tag{12}$$

as rearranged from eq 8. The fitted values for j^0_{water} and (c_1 cos α)/RT are 4.8(3) × 10^{-4} mA and 11.02(4), respectively (standard deviations in parentheses). From the latter value, c_1 cos α = 6.3 kcal nm mol^{-1} V^{-1} is obtained at T = 288 K.

To describe the local conditions at the phase boundary, it must be taken into account that a double layer with a characteristic Debye length and dielectric constant ϵ_{dl} is formed at the oxide−electrolyte interface. From the continuity requirement of the normal component of the electric displacement at the oxide/electrolyte interface, and neglecting the effect of specific ionic adsorption,[24] the following correction for F, the field strength in the double layer, is obtained:

$$F \approx \frac{U}{d_C} \frac{\varepsilon_{Al_2O_3}}{\varepsilon_{dl}} \tag{13}$$

It is well-established in electrochemistry that, at an interface with a solid, the dielectric permittivity (ϵ) of water is not the same as that in the bulk liquid. Rather, ϵ has its smallest value ϵ_{min} (ca. 4−6) at the first layer at the water/solid interface and increases with the distance from the surface, up to ϵ_{max} = 78 in the bulk[25−27]

$$\varepsilon(z) = \varepsilon_{max}[1 + (\varepsilon_{max}/\varepsilon_{min} - 1)\exp(-z/L^{-1})]^{-1} \tag{14}$$

where z is the distance from the surface and L^{-1} is the Debye length related to the double layer in a given electrolyte. According to the Debye−Hückel theory, the Debye length is given as

$$L^{-1} = \sqrt{\frac{\varepsilon_0 \varepsilon_r k_B T}{e^2 \sum n_i^{\infty} Z_i^2}} \tag{15}$$

where ϵ_0 and ϵ_r are the vacuum permittivity and the relative permittivity of the bulk electrolyte, respectively, k_B is the Boltzmann constant, T the absolute temperature, e the electronic unit charge, n' the ion density in the bulk solution, and Z_i the ion valency. The sum runs over all species of ions present. In the present work for the electrolyte of 0.3 M oxalic acid with a pH = 1.2, the calculated thickness of the Debye length is about 1.2 nm. In agreement with previous work[25,26b] we find that such a Debye length of ca. 1 nm corresponds to a dielectric constant of about 6 of the electrolyte at the oxide and electrolyte interface (this ϵ value was also employed for the polarizable continuum in the quantum-chemical computations discussed above). A plot of the dielectric permittivity of the electrolyte as a function of the distance from the surface is shown in Figure S1 in the Supporting Information. Together with the permittivity of the bulk oxide taken as $\epsilon_{Al2O3} \approx 9$, a refined empirical estimate for $c_1$cos α = 4.2 kcal nm mol^{-1} V^{-1} is obtained.

A further refinement of the local field strengths at the sites of the adsorbed water molecules is possible by considering that in a pure dielectric, this local field will be increased due to the response of the dielectric to the external field (i.e., due to the polarization of the medium). For example, in a spherical cavity within a uniform dielectric, the local field F_{loc} is related to the external field F_{ext} by[25]

$$F_{loc} = F_{ext} 3\varepsilon/(2\varepsilon + 1) \tag{16}$$

Thus, F_{loc} is enhanced by a factor approaching 1.5 in very polar environments. For ϵ = 6, the empirical estimate for c_1 cos α would be multiplied by (2ϵ + 1)/3ϵ = 0.722, resulting in a value of 3.03 kcal nm mol^{-1} V^{-1} for this quantity. This value is now in between the upper limit and the value corresponding to α = 54° modeled

(22) Ono, S.; Saito, M.; Ishiguro, M.; Asoh, H. *J. Electrochem. Soc.* **2004**, *151*, B473–B478.
(23) (a) Lee, W.; Ji, R.; Gösele, U.; Nielsch, K. *Nat. Mater.* **2006**, *5*, 741–747. (b) Hunter, M. S.; Fowle, P. *J. Electrochem. Soc.* **1954**, *101*, 481–485.
(24) Parkhutik, V. P.; Shershulsky, V. I. *J. Phys. D: Appl. Phys.* **1992**, *25*, 1258–1263.
(25) Bockris, J.O'M.; Reddy, A. K. N. *Modern Electrochemistry*; Plenum Press: New York, 1970.
(26) (a) Teschke, O.; Ceotto, G.; de Souza, E. F. *Chem. Phys. Lett.* **2000**, *326*, 328–334. (b) Teschke, O.; Ceotto, G.; de Souza, E. F. *Phys. Rev. E* **2001**, *64*, 011605.
(27) Cherepanov, D. A.; Feniouk, B. A.; Junge, W.; Mulkidjanian, A. Y. *Biophys. J.* **2003**, *85*, 1307–1316.

computationally (see dotted line in Figure 5).[28] In view of the many assumptions and approximations that are involved, this apparent semiquantitative accordance between theory and experiment should probably not be overinterpreted. Nevertheless, both are in excellent qualitative agreement as to the order of magnitude of the underlying effect. Our results thus can be taken as strong evidence for the proposed models of equifield strength and field-enhanced dissociation of water at the growing oxide surface.

Conclusion

In summary, we have shown using quantum-chemical model computations that an external electric field can facilitate the heterolytic dissociation of properly oriented water molecules significantly. This fundamental finding strongly supports a previously proposed new mechanistic model for the electrochemical formation of porous aluminum oxide, which accounts for the decreasing porosity of the product with increasing applied voltage. Assuming that suitable orientations of water molecules are brought about by adsorption at the oxide surface, and employing physically reasonable relations between macroscopic and local electric field strengths, a remarkably good accord is found between key quantities derived from the quantum-chemical models and the experimental data. Arguably, this conceptual link between the fundamental response of a molecule to an external stimulus and the property of a material that is of interest for technological applications holds much promise for further exploration.

Acknowledgment. This work was supported by EPSRC and EaStChem via the EaStChem Research Computing facility. M.B. thanks Dr. H. Früchtl for technical assistance.

Supporting Information Available: Additional graphical material, full citation of ref 14, and optimized geometries and energies in form of Gaussian archive entries. This material is available free of charge via the Internet at http://pubs.acs.org.

JA902267B

(28) Since the computations involved both an external field and a dielectric continuum, they have implicitly used the corresponding local field.